Colloids and Surfaces B: Biointerfaces 167 (2018) 150–155

Contents lists available at ScienceDirect

Colloids and Surfaces B: Biointerfaces

journal homepage: www.elsevier.com/locate/colsurfb

DNA-functionalized gold nanoparticle-based fluorescence polarization for the sensitive detection of silver ions

Gongke Wang [a,*], Shuangli Wang [a], Changling Yan [a], Guangyue Bai [a], Yufang Liu [b,**]

[a] School of Chemistry and Chemical Engineering, Key Laboratory of Green Chemical Media and Reactions, Ministry of Education, Collaborative Innovation Center of Henan Province for Green Manufacturing of Fine Chemicals, Henan Normal University, Xinxiang, Henan, 453007, PR China
[b] School of Physics and Materials Science, Henan Normal University, Xinxiang, Henan, 453007, PR China

ARTICLE INFO

Article history:
Received 12 January 2018
Received in revised form 29 March 2018
Accepted 2 April 2018
Available online 5 April 2018

Keywords:
Gold nanoparticle
Fluorescence polarization
Biosensor
Ag^+ detection

ABSTRACT

Despite their practical applications, Ag^+ ions are environmental pollutants and affect human health. So the effective detection methods of Ag^+ ions are imperative. Herein, we developed a simple, sensitive, selective, and cost-effective fluorescence polarization sensor for Ag^+ detection in aqueous solution using thiol-DNA-functionalized gold nanoparticles (AuNPs). In this sensing strategy, Ag^+ ions can specifically interact with a cytosine–cytosine (C—C) mismatch in DNA duplexes and form stable metal-mediated cytosine–Ag^+–cytosine (C–Ag^+–C) base pairs. The formation of the C–Ag^+–C complex results in evident changes in the molecular volume and fluorescence polarization signal. To achieve our aims, we prepared two complementary DNA strands containing C-base mismatches (probe A: 5′-SH-A_{10}-TACCACTCCTCAC-3′ and probe B: 5′-TCCTCACCAGTCCTA-FAM-3′). The stable hybridization between probe A and probe B occurs with the formation of the C–Ag^+–C complex in the presence of Ag^+ ions, leading to obvious fluorescence quenching in comparison to the system without AuNP enhancement. The assay can be used to identify nanomolar levels of Ag^+ within 6 min at room temperature, and has extremely high specificity for Ag^+, even in the presence of higher concentrations of interfering metal ions. Furthermore, the sensor was successfully applied to the detection of Ag^+ ions in environmental water samples and showed excellent selectivity and high sensitivity, implying its promising application in the future.

1. Introduction

Ag^+ ions have excellent antibiotic and bactericidal effects. They also have wide uses in the fields of photography, video, electronics, pharmaceuticals, biosensing, etc. However, Ag^+ ions are considered hazardous metal ions and are a major environmental pollutant. Furthermore, they can destroy the activity of enzymes and combine with amine, imidazole, and various metabolites, with negative consequences for environmental safety and human health [1–7]. Owing to these adverse effects, the development of a rapid and simple method for Ag^+ detection is imperative. Conventional methods, such as flame atomic absorption, potentiometry, voltammetry, inductively coupled plasma atomic emission spectrometry, and fluorescence methods, are widely used to detect Ag^+ ions. However, these methods have various shortcomings, e.g., they are generally time-consuming, expensive, and complicated [8–12]. Therefore, it is imperative to develop a sensitive and selective biosensor for Ag^+ ion detection [13–16].

In the last few decades, extensive efforts have focused on the design of sensing systems for the detection of Ag^+ ions, including sensors based on fluorescent chromophores [17], semiconductor quantum dots [18,19], colorimetric sensors [20,21], and fluorescent sensors [22,23]. However, many of these systems have major limitations, such as interference from closely related metal ions, high costs, and complicated analytical procedures. Recently, the high specificity of the interaction of oligonucleotides with metal ions has been successfully and widely used for studies of heavy metal ion detection. Since Ono et al. first found that Ag^+ can selectively coordinate cytosine (C) bases to form a stable C–Ag^+–C complex, an assay based on the specific coordination of Ag^+ with C bases has been widely employed for monitoring Ag^+ ions [24]. Zhao et al. reported a reusable DNA single-walled carbon nanotube-based fluorescent sensor for the highly sensitive and selective detection of Ag^+ and cysteine (Cys) in aqueous solution. This approach enabled the simultaneous detection of two objects, but the detection range was relatively narrow [25]. Lv et al. described a reversible fluores-

* Corresponding author at: School of Chemistry and Chemical Engineering, Henan Normal University, 46 Jian-she Road, Mu Ye District, Xinxiang, 453007, PR China.
** Corresponding author.
E-mail addresses: wanggongke@126.com (G. Wang), yf-liu@htu.cn (Y. Liu).

https://doi.org/10.1016/j.colsurfb.2018.04.004
0927-7765/

cent DNA–based INHIBIT logic gate for the determination of Ag^+ and I^-. In this method, graphene oxide was used as a signal transducer and Ag(I) and iodide as mechanical activators. Although this biosensor was highly sensitive with low background interference, highly toxic AgI was introduced in this system [26].

Sensors based on gold nanoparticles (AuNPs) are promising for the simple and rapid tracking of Ag^+ based on the extreme sensitivity of the surface plasmon resonance absorbance of AuNPs [27–29]. For example, Lin et al. reported a colorimetric method for the detection of Hg^{2+} and Ag^+ using Tween 20-modified AuNPs [30]. Li et al. developed both unlabeled and labeled sensing strategies for Ag^+ ions using the DNA-based AuNPs colorimetric strategy [31]. However, these two approaches are susceptible to severe interference from other metal ions and typically require masking agents. These masking agents are often highly toxic, resulting in additional environmental contamination and complicated analytical procedures. Likewise, an on–off sensor based on DNA-functionalized AuNPs for silver ions and cysteine detection using a light-scattering technique has been generated, but a satisfactory limit of detection (LOD) has not been obtained [32]. Zhou et al. designed a novel biosensor based on nanoporous gold and duplex-like DNA scaffolds with an anionic intercalator to realize Ag^+ ion detection [33]. Additionally, an AuNP and enzyme cleavage-based dual signal amplification strategy for ultrasensitive detection of Ag^+ using electrochemical techniques has been proposed by Miao et al. [34]. These sensing platforms for Ag^+ detection have extremely low LODs and high selectivity over other environmentally relevant metal ions, but require expensive instruments and complex procedures. Thus, the development of a highly sensitive, simple, rapid, and cost-effective assay for Ag^+ ion detection remains a challenge.

Inspired by previous reports, we proposed a simple, rapid, and highly selective sensor for the detection of Ag^+ using cytosine–Ag^+–cytosine (C–Ag^+–C) coordination chemistry and a fluorescence polarization technique enhanced by AuNPs and optimized the experimental conditions. This novel sensor is very simple and cost-effective, and can identify Ag^+ at the nanomolar level (LOD = 9.5 nM) using widely available materials and instruments at room temperature. In addition, the analysis procedure is very rapid, which only takes approximately 6 min to achieve Ag^+ detection. Moreover, in the presence of other competitive metal ions, this biosensor is highly selective for Ag^+ without masking agents, minimizing additional environmental pollution. Most important, the proposed strategy may have broad applications for the monitoring of other metal ions by applying different DNA strands of specific sequences.

2. Materials and methods

2.1. Materials and instruments

All chemicals used in this work were obtained from commercial sources and used directly, without further purification. Trisodium citrate and hydrogen tetrachloroaurate (III) hydrate ($HAuCl_4{\cdot}3H_2O$, purity ≥ 99.9%) were purchased from Sigma (St. Louis, MO, USA). Probe A (5′-SH-A_{10}-TACCACTCCTCAC-3′) and probe B (5′-TCCTCACCAGTCCTA-FAM-3′) were synthesized using a standard procedure and purified by reverse-phase high-performance liquid chromatography by Sangon Inc. (Shanghai, China). Silver nitrate ($AgNO_3$, purity ≥ 99.5%), sodium nitrate ($NaNO_3$, purity ≥ 99.9%), and tris-(2-carboxyethyl) phosphine hydrochloride (TCEP, purity ≥ 99%) were purchased from Alfa Aesar (Haverhill, MA, USA). $AgNO_3$ was weighed to prepare a stock solution, which was diluted to the desired concentrations for the experiments. The concentration of the $AgNO_3$ solution was calibrated by atomic absorption spectrophotometry. Other metal ions were of analytical grade and were purchased from Shanghai Sinopharm (Shanghai, China). Water used in all experiments was double-distilled.

Fluorescence polarization was performed using a Cary Eclipse Fluorescence Spectrophotometer equipped with a normal polaroid (Varian, Palo Alto, CA, USA). UV–vis spectra were recorded on a TU-1810 spectrophotometer (Puxi Analytic Instrument Ltd., Shanghai, China). Transmission electron microscopy (TEM) images were obtained using a JEM 2100 (JEOL, Tokyo, Japan) operated at 200 kV. Flame atomic absorption spectroscopy results were recorded using the aZ-5000 Flame Atomic Absorption Spectrophotometer (Hitachi, Tokyo, Japan). Centrifugation was performed using a high-speed refrigerated centrifuge (Shanghai Anting Scientific Instrument Co., Ltd., Shanghai, China). All pH measurements were obtained using a Model pHS-2C pH meter (Shanghai Dapu Instrument Co., Ltd., Shanghai, China). Temperature was maintained in a low-temperature thermostat bath (Shanghai Ping Xuan Science Instrument Co., Ltd., Shanghai, China).

2.2. Synthesis and functionalization of AuNPs

Citrate-capped AuNPs were prepared by the chemical reduction of $HAuCl_4{\cdot}3H_2O$ in the liquid phase [6]. All glassware was cleaned in aqua regia and rinsed with double-distilled water prior to use. A 0.01% $HAuCl_4$ solution (100 mL) was brought to a vigorous boil with stirring in a round-bottom flask fitted with a reflux condenser, and 3.5 mL of 1% trisodium citrate solution was rapidly added to the boiling solution. Finally, the mixture was heated under reflux for another 15 min. During this time, the mixture changed from pale yellow to deep red. The mixture was cooled to room temperature, while stirring continuously. Then, it was filtered through a 0.45-μm membrane filter and stored in a refrigerator at 4 °C. AuNPs were nearly monodispersed, and the average size was 13 ± 2 nm based on a TEM analysis. The concentration of AuNPs was evaluated by UV–vis spectroscopy using an extinction coefficient of $2.7 \times 10^8\ M^{-1}\ cm^{-1}$ at λ = 520 nm (Fig. 1) [35].

Before the functionalization of AuNPs, probe oligonucleotides were deprotected by soaking in 20 mM Tris-CH_3COOH buffer solution (pH 7.0) containing 100 mM TCEP for at least 2 h. AuNPs were functionalized with the probe A following the normal procedure. The solution was incubated at 25 °C for 12 h in 10 mM Tris-CH_3COOH (pH 7.0). Then, the NaCl solution was gradually added, and the final concentration of NaCl was 0.1 M. Finally, the solution was allowed to "age" under these conditions for an additional 24 h to form DNA–AuNPs complexes. Excess reagents were removed by centrifugation at 21,560 × *g* (14,000 rpm) and 4 °C for at least 20 min. Following removal of the supernatants, the oily precipitates were washed with 10 mM Tris-CH_3COOH (pH 7.0). After three centrifuge/wash cycles, the colloidal solution was suspended in stock solution and placed in a refrigerator until further use. Before each experiment, the UV–vis absorbance of the stock solution of DNA–AuNPs was determined, and the constant absorption spectrum confirmed the stability of DNA-AuNPs.

2.3. Effect of gold nanoparticles on probe B

AuNPs (50 nM) were added to the probe B solution, and the fluorescence polarization values of the mixed solution and single probe B solution were measured at an excitation wavelength of 485 nm. The effect of AuNPs on the fluorescence polarization value of the probe B solution was evaluated.

2.4. Fluorescence polarization measurements

The prepared AuNP-DNA and probe B solutions were mixed with equal volumes, and then the $AgNO_3$ standard solution was added to

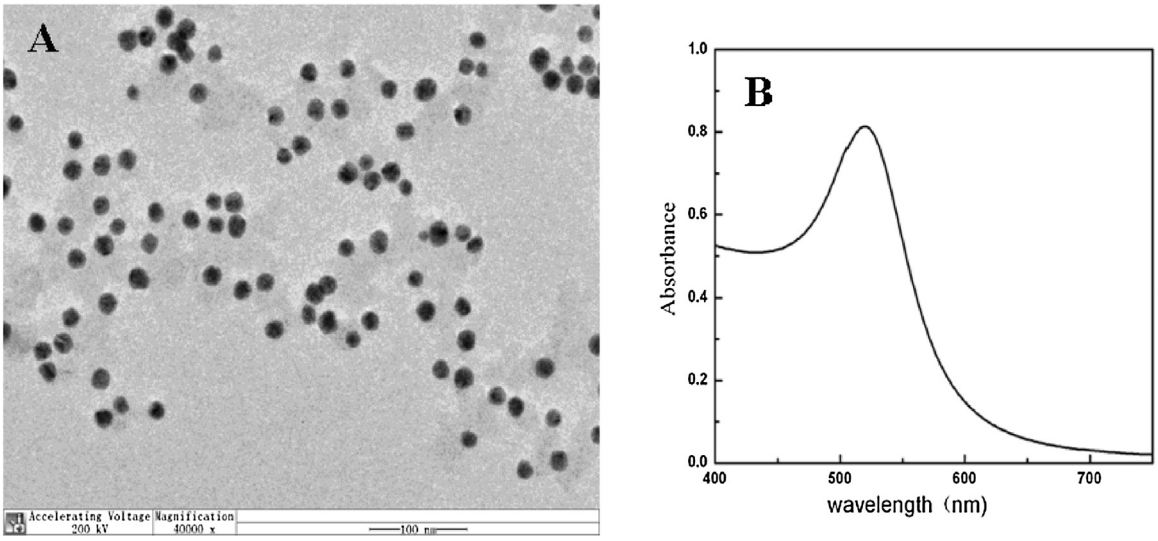

Fig. 1. (A) TEM images of AuNPs and (B) UV–vis absorption spectra of AuNPs.

the mixture. The fluorescence polarization values *FP* of the samples were recorded using a Cary Eclipse Fluorescence Spectrophotometer.

2.5. Analysis of real samples

A series of samples were prepared by spiking locally obtained tap water with standard solutions of Ag^+ (50–700 nM). These spiked samples were added to a solution containing 10 nM AuNP–DNA and 1 μM probe B (Tris-CH_3COOH buffer solution, pH 7.0). After incubation for 30 min, fluorescence polarization changes ΔFP were estimated using a Cary Eclipse Fluorescence Spectrophotometer at room temperature.

3. Results and discussion

3.1. Sensing strategy

The fluorescence polarization value *FP* is sensitive to changes in the rotational motion of fluorescently labeled molecules. The fluorescence polarization value *FP* can typically be estimated using the Perrin equation as follows [36]:

$$\frac{1}{FP} = \frac{1}{FP_0} + \left(\frac{1}{FP_0} - \frac{1}{3}\right)\frac{RT\tau}{V\eta}, \quad (1)$$

where τ is the fluorescence lifetime, η is the viscosity of the solution, *T* is the absolute temperature, *R* is the gas constant, *V* is the volume of the rotating unit, and FP_0 is the limiting polarization. The *FP* value of a fluorophore is proportional to its rotational relaxation time, which in turn depends on its molecular volume or molecular weight. It is known that smaller molecules rotate faster and hence possess smaller *FP* values. In contrast, larger molecules are expected to have greater *FP* values owing to the slower rotation rate [37–39].

The principle of the method is illustrated in Scheme 1. We first prepared two complementary DNA strands containing a cytosine base (C-base) mismatch, probe A (5′-SH-A_{10}-TACCACTCCTCAC-3′) and probe B (5′-TCCTCACCAGTCCTA-FAM-3′). Probe A was modified on the surface of AuNPs. Probe B was labeled with the fluorescence chromophore FAM. In the presence of Ag^+ ions, the stable pairing between probe A and probe B (two DNA chains with a partial C—C mismatch) occurs with the formation of the C–Ag^+–C complex, resulting in the stable binding of fluorophore-labeled probe B to the surface of AuNPs. Consequently, the molecular volume increases and the relaxation time increases, thus substantially increasing the *FP* value. Therefore, the quantitative detection of silver ions can be achieved by this strategy.

3.2. Optimization of the general procedure

3.2.1. Effect of gold nanoparticles on the fluorescence polarization value of probe B

As shown in Fig. S1, in Tris-CH_3COOH buffer solution (pH = 7.0), the fluorescence polarization values *FP* of the pure probe B solution and the probe B solution with a large amount of AuNPs were similar, indicating that the quenching properties of AuNPs do not affect fluorescence polarization after the addition of the probe B solution. Because fluorescence polarization is related to the molecular size of the fluorescent substance, mismatched double-stranded DNA exhibits complementary pairing in the presence of Ag^+, and AuNPs are attached to the fluorescent molecules; accordingly, it is feasible to quantitatively detect of silver ions based on a change in the molecular size of the fluorescent substance.

3.2.2. Effect of $NaNO_3$ on the fluorescence polarization value

Fig. S2 shows the effect of $NaNO_3$ on the fluorescence polarization value *FP*. AuNPs-DNA and the probe B solution were mixed in 50 mM Tris-CH_3COOH buffer solution (pH = 7.0), and 100 nM $AgNO_3$ solution was added using various concentrations of $NaNO_3$ (10, 20, 30, 50, 70, 100, 150, and 200 mm). As shown in Fig. S2, when the concentration of $NaNO_3$ was in the range of 0–50 mM, the *FP* value gradually increased as the $NaNO_3$ concentration increased, and this may be explained by the increase in ionic strength, which is beneficial to the hybridization of the DNA chain. Additionally, the changes in fluorescence polarization values reached a plateau when the concentration of $NaNO_3$ solution was 50 mM, after which little changes in the fluorescence polarization values were detected. Therefore, the optimal concentration of $NaNO_3$ was 50 mM, and this concentration was used in subsequent experiments.

3.2.3. Effect of temperature on the fluorescence polarization value

Temperature affects the fluorescence polarization value [39]. To determine the optimal temperature for the sensing system, the fluorescence polarization value *FP* was measured at temperatures ranging from 15 °C to 55 °C. The results are presented in Fig. S3. An increase in temperature is favorable for the formation of double-stranded DNA in the range of 15 °C–25 °C, and the fluorescence

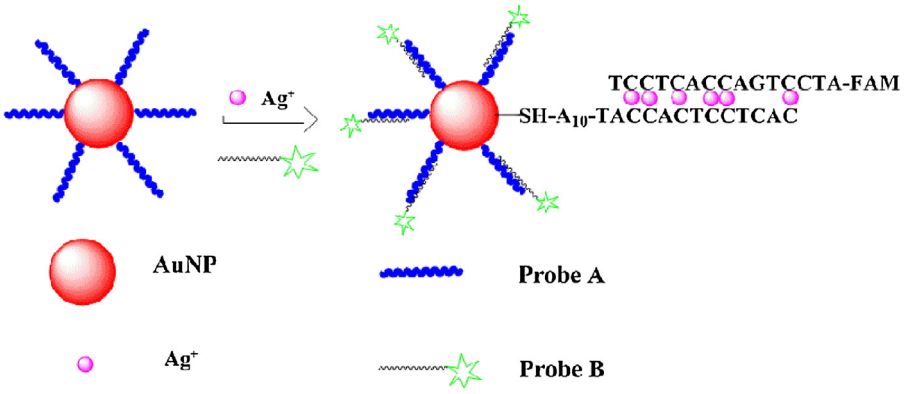

Scheme 1. Schematic illustration of the assay for the detection of Ag^+.

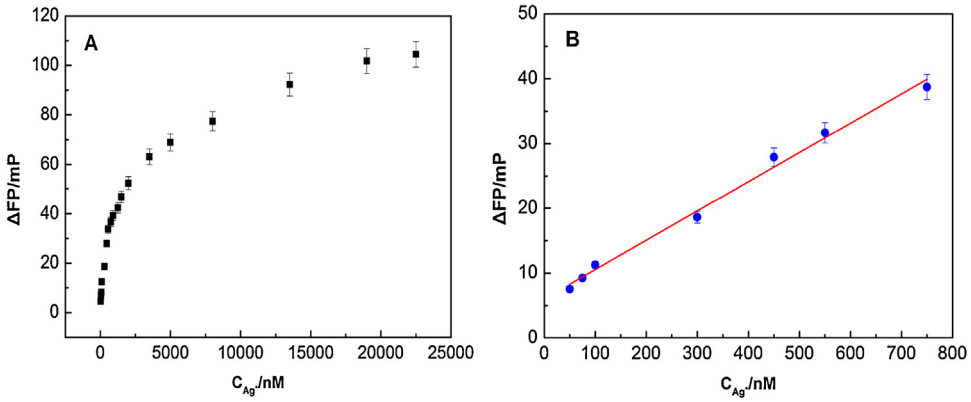

Fig. 2. (A) Change in fluorescence polarization (ΔFP) of AuNPs-DNA-FAM upon the addition of various concentrations of Ag^+; (B) Linear correlation between the change in the fluorescence polarization value (ΔFP) and the concentration of Ag^+ (50–750 nM). All measurements were performed in a 50 mM Tris-CH_3COOH buffer solution (pH 7.0). Data represent the average values of three measurements (n = 3); the error bars are signed according to the measurement maximal deviation (5%).

polarization value increased as the temperature increased within this range. As the temperature continued to increase, molecular motion is accelerated and the relaxation time is reduced, resulting in a gradual reduction in the fluorescence polarization value. Apparently, 25 °C was the optimal temperature and was used for all subsequent experimental procedures.

3.2.4. *Effect of pH on the fluorescence polarization value*

The appropriate pH is critical for an effective sensing system for silver ions [37]. Generally, a low pH value is not conducive to the formation of stable double-stranded DNA, but a high pH value often hampers the formation of C–Ag^+–C base pairs. As summarized in Fig. S4, in the pH range of 4.0–7.0, the fluorescence polarization value *FP* increased gradually as the pH increased. However, when pH values were 7.0–10.0, the fluorescence polarization value clearly decreased as pH increased. In a partial alkaline environment, Ag^+ tends to form hydroxide, and C–Ag^+–C complex formation may be difficult. Consequently, pH = 7.0 is optimal for this sensing system.

3.3. *Analysis of the dynamics of silver ions*

To estimate the performance and unique properties of the proposed biosensor, the kinetics of Ag^+ detection using the fluorescence polarization technique was investigated. As shown in Fig. S5, the fluorescence polarization value *FP* increased continuously with an increase in the reaction time from 0 to 5 min and reached equilibrium after 6 min. These observations confirmed that the detection of Ag^+ using the fluorescence polarization method is rapid. Therefore, the strategy proposed here is useful for the sensitive and selective detection of Ag^+.

3.4. *Sensitivity*

Under optimized conditions, we tested the sensitivity of the sensing system toward Ag^+. Fig. 2 displays the fluorescence polarization changes ΔFP of probe B for various concentrations of Ag^+. For an excitation wavelength of 485 nm, the biosensor had an emission peak at 518 nm, and the change in the fluorescence polarization value ΔFP increased as the Ag^+ concentration increased, implying that the addition of Ag^+ promotes complementary pairing of probe B and probe A. The fluorescently labeled molecule increases gradually with the formation of the DNA double chain, resulting in an increase in the fluorescence polarization value. Thus, the quantitative detection of Ag^+ is possible based on the change in the fluorescence polarization value ΔFP. As demonstrated in Fig. 2A, when the concentration of Ag^+ was less than 3500 nM, the difference in fluorescence polarization increased progressively for increasing Ag^+ concentrations. However, when the Ag^+ concentration was greater than 3500 nM, the difference in fluorescence polarization changed little and reached a plateau, indicating the binding equilibrium and saturation interaction of Ag^+ with probe A and probe B. Fig. 2B illustrates the calibration curve for the detection of Ag^+ based on the proposed biosensor. A linear correlation between the change in the fluorescence polarization value ΔFP and the concentration of Ag^+ was observed in the concentration range of 50–750 nM. The linear regression equation is $y = (0.0452 \pm 0.0017)x + (6.028 \pm 0.706)$ with the correlation coefficient $R^2 = 0.9913$. At a signal-to-noise ratio of 3, the limit of detection (LOD) for Ag^+ was

Table 1
Comparison of the proposed method with other sensors based on AuNPs for the detection of Ag^+ ions.

Method of detection	Linear range	Limit of detection	Reference
Benzo crown-ether modified AuNPs	20–950 nM	12.5 nM	[21]
Cytidine-stabilized gold nanocluster	0.01–6 μM	10 nM	[22]
Au-Ag core-shell NPs	1.09–109 nM	1.09 nM	[29]
Tween 20-stabilized AuNPs	400–1000 nM	100 nM	[30]
Labeled DNA-AuNPs	0–29.5 μM	0.59 nM	[31]
DNA-functionalized AuNPs	250–700 nM	50 nM	[32]
SH-DNA functionalized AuNPs	50–750 nM	9.5 nM	This work

estimated to be 9.5 nM, which was much lower than the standard for Ag^+ in drinking water recommended by the Environmental Protection Agency [28]. A comparison of the biosensor in this work with other published methods based on AuNPs for the detection of Ag^+ ions is presented in Table 1. It is shown that our method has a lower detection limit for Ag^+ ions without using masking agents and the complex procedures, suggesting its potential application for the sensitive detection of Ag^+ in aqueous solution.

3.5. Selectivity

To test the selectivity of the developed biosensor, the assay was applied using other environmentally relevant metal ions, including Ca^{2+} and Mg^{2+} (both 1 mM), and Cu^{2+}, Zn^{2+}, Ni^{2+}, Mn^{2+}, Co^{2+}, K^+, and Al^{3+} (each 1 μM), and the responses were investigated under the same conditions used in the case of Ag^+. The results are presented in Fig. 3. The addition of Ag^+ (100 nM) caused a remarkable change in fluorescence polarization *FP*. However, there was very little increase in the fluorescence polarization value *FP* in the presence of other metal ions. This observation revealed that Ag^+ ions can specifically interact with cytosine bases to form strong and stable C–Ag^+–C complexes, indicating that the sensing system provided excellent specificity and selectivity for the detection of Ag^+ against other interfering metal ions at higher concentrations.

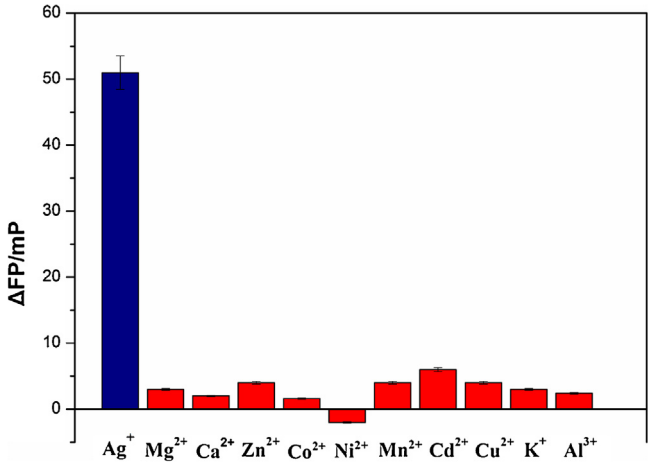

Fig. 3. Metal ion-induced fluorescence polarization changes (Δ*FP*) for AuNP-DNA-FAM in 50 mM Tris-CH_3COOH at pH 7.0. Concentrations of metal ions: Ca^{2+} and Mg^{2+} (both 1 mM), Cu^{2+}, Zn^{2+}, Ni^{2+}, Mn^{2+}, Co^{2+}, Cd^{2+}, K^+, and Al^{3+} (each 1 μM). Data represent the average values of three measurements (n = 3); the error bars are signed according to the measurement maximal deviation (4%).

Table 2
Detection of Ag^+ in water samples spiked with specific interfering ions using the proposed biosensor (n = 3).

Samples	Mean observed (nM)	Mean recovery[a] (%)	RSD[c] (%)
Ag^+[b] (60.0 nM), Ca^{2+} and Mg^{2+} (both 1.0 mM), Cu^{2+}, Zn^{2+}, Ni^{2+}, Mn^{2+}, Co^{2+}, Cd^{2+}, K^+, and Al^{3+} (each 1.0 μM)	58.7	97.8	1.67
Ag^+[b] (150.0 nM), Ca^{2+} and Mg^{2+} (both 1.0 mM), Cu^{2+}, Zn^{2+}, Ni^{2+}, Mn^{2+}, Co^{2+}, Cd^{2+}, K^+, and Al^{3+} (each 1.0 μM)	153.4	102.3	2.14
Ag^+[b] (450.0 nM), Ca^{2+}, and Mg^{2+} (both 1.0 mM), Cu^{2+}, Zn^{2+}, Ni^{2+}, Mn^{2+}, Co^{2+}, Cd^{2+}, K^+, and Al^{3+} (each 1.0 μM)	457.3	101.6	1.82
Ag^+[b] (700.0 nM), Ca^{2+} and Mg^{2+} (both 1.0 mM), Cu^{2+}, Zn^{2+}, Ni^{2+}, Mn^{2+}, Co^{2+}, Cd^{2+}, K^+, and Al^{3+} (each 1.0 μM)	692.1	98.9	0.85

[a] Mean recovery (%) = 100 × ($C_{meanobserved}$/$C_{standard}$).
[b] Ag^+, concentration of Ag^+ standard solution.
[c] RSD, relative standard deviation.

3.6. Sensor application

The sensor constructed here is expected to be applicable to real environmental water owing to the favorable sensitivity and selectivity. To reveal the practical applicability of this sensor, it was used to detect Ag^+ in tap water samples. These water samples did not contain Ag^+ according to a flame atomic absorption spectrophotometer; therefore, a standard solution of Ag^+ and some additional metal ions were manually added to simulate contaminated water. The results show good agreement with the expected and observed values, as summarized in Table 2. The mean recoveries of these samples were between 97.8% and 102.3%. These results clearly demonstrate that the proposed biosensor is able to detect Ag^+ in environmental water samples with high sensitivity and excellent selectivity.

4. Conclusions

In summary, we developed a new assay for the selective detection of Ag^+ at room temperature using a fluorescence polarization technique and AuNPs. The assay is based on cytosine–Ag^+–cytosine coordination chemistry; the labeled DNA and the complementary DNA strand modified with AuNPs are fully paired in the presence of Ag^+. Additionally, we optimized temperature, salt concentration, pH, and other conditions, and explored the kinetic process of silver ion detection using the fluorescence polarization method. The novel sensing strategy is simple, rapid, and highly selective. Moreover, it can be easily extended to detect other heavy metal ions, antibodies, small molecules, and proteins. For example, antibodies can be detected by interactions with specific antigens, other heavy metal ions can be monitored using targeted oligonucleotides, and small molecule detection can be achieved based on specific binding to the DNA. Therefore, this detection method has potentially wide applications and accordingly is worthy of further research.

Acknowledgements

This work was supported by the Program for Innovative Research Team in University of Henan Province (18IRTSTHN003), the China Postdoctoral Science Foundation (2016M592292), the

National Natural Science Foundation of China (21773059 and 21303043), the Science and Technology Innovation Talent Project of Xinxiang, China (CXRC16005).

Appendix A. Supplementary data

Supplementary data associated with this article can be found, in the online version, at https://doi.org/10.1016/j.colsurfb.2018.04.004.

References

[1] Y. Wei, B. Li, X. Wang, Y. Duan, Magnified fluorescence detection of silver (I) ion in aqueous solutions by using nano-graphite-DNA hybrid and DNase I, Biosens. Bioelectron. 58 (2014) 276–281.
[2] Y. Cao, W. Wu, S. Wang, H. Peng, X. Hu, Y. Yu, Monolayer g-C3N4 fluorescent sensor for sensitive and selective colorimetric detection of silver ion from aqueous samples, J. Fluoresc. 26 (2016) 739–744.
[3] G. Yan, Y. Wang, X. He, K. Wang, J. Su, Z. Chen, Z. Qing, A highly sensitive electrochemical assay for silver ion detection based on un-labeled C-rich ssDNA probe and controlled assembly of MWCNTs, Talanta 94 (2012) 178–183.
[4] G. Xu, G. Wang, X. He, Y. Zhu, L. Chen, X. Zhang, An ultrasensitive electrochemical method for detection of Ag^+ based on cyclic amplification of exonuclease III activity on cytosine–Ag^+–cytosine, Analyst 138 (2013) 6900–6906.
[5] O. Choi, Z. Hu, Size dependent and reactive oxygen species related nanosilver toxicity to nitrifying bacteria, Environ. Sci. Technol. 12 (2008) 4583–4588.
[6] T. Lou, Z. Chen, Y. Wang, L. Chen, Blue-to-red colorimetric sensing strategy for Hg^{2+} and Ag^+ via redox-regulated surface chemistry of gold nanoparticles, ACS Appl. Mater. Interfaces 3 (2011) 1568–1573.
[7] P. Miao, Y.G. Tang, L. Wang, DNA modified Fe3O4@Au magnetic nanoparticles as selective probes for simultaneous detection of heavy metal ions, ACS Appl. Mater. Interfaces 9 (2017) 3940–3947.
[8] M. Ghaedi, A. Shokrollahi, K. Niknam, E. Niknam, A. Najibi, M. Soylak, Cloud point extraction and flame atomic absorption spectrometric determination of cadmium (II) lead (II), palladium (II) and silver (I) in environmental samples, J. Hazard. Mater. 168 (2009) 1022–1027.
[9] W.Y. Xie, W.T. Huang, N.B. Li, H.Q. Luo, Design of a dual-output fluorescent DNA logic gate and detection of silver ions and cysteine based on graphene oxide, Chem. Commun. 48 (2012) 82–84.
[10] A. Afkhami, A. Shirzadmehr, T. Madrakian, H. Bagheri, New nano-composite potentiometric sensor composed of graphene nanosheets/thionine/molecular wire for nanomolar detection of silver ion in various real samples, Talanta 131 (2015) 548–555.
[11] S. Zhan, H. Xu, X. Zhan, Y. Wu, L. Wang, J. Lv, P. Zhou, Determination of silver (I) ion based on the aggregation of gold nanoparticles caused by silver-specific DNA, and its effect on the fluorescence of Rhodamine B, Microchim. Acta 182 (2015) 1411–1419.
[12] K. Ndung'u, M.A. Ranville, R.P. Franks, A.R. Flegal, On-line determination of silver in natural water by inductively-coupled plasma mass spectrometry: influence of organic matter, Mar. Chem. 98 (2006) 109–120.
[13] M. Ebrahimi, J.B. Raoof, R. Ojani, Novel electrochemical DNA hybridization biosensors for selective determination of silver ions, Talanta 144 (2015) 619–626.
[14] X. Ran, H. Sun, F. Pu, J. Ren, X. Qu, Ag nanoparticle-decorated graphene quantum dots for label-free, rapid and sensitive detection of Ag^+ and biothiols, Chem. Commun. 49 (2013) 1079–1081.
[15] Y. Yang, S. Zhang, M. Kang, L. He, J. Zhao, H. Zhang, Z. Zhang, Selective detection of silver ions using mushroom-like polyaniline and gold nanoparticle nanocomposite-based electrochemical DNA sensor, Anal. Biochem. 490 (2015) 7–13.
[16] K. Mao, Z. Wu, Y. Chen, X. Zhou, A. Shen, J. Hu, A novel biosensor based on single-layer MoS2 nanosheets for detection of Ag^+, Talanta 132 (2015) 658–663.
[17] L. Liu, G. Zhang, J. Xiang, D. Zhang, D. Zhu, Fluorescence turn on chemosensors for Ag^+ and Hg^{2+} based on tetraphenylethylene motif featuring adenine and thymine moieties, Org. Lett. 10 (2008) 4581–4584.
[18] T. Gong, J. Liu, X. Liu, J. Liu, J. Xiang, Y. Wu, A sensitive and selective sensing platform based on CdTe QDs in the presence of L-cysteine for detection of silver, mercury and copper ions in water and various drinks, Food Chem. 213 (2016) 306–312.
[19] Y. Song, T. Tang, X. Wang, G. Xu, F. Wei, Y. Wu, Q. Song, Y. Ma, Y. Ma, Y. Cen, Q. Hu, Highly selective and sensitive detection of adenosine utilizing signal amplification based on silver ions-assisted cation exchange reaction with CdTe quantum dots, Sens. Actuators B 247 (2017) 305–311.
[20] C. Li, Y. Yang, B. Zhang, G. Chen, Z. Wang, G. Li, Conjugation of graphene oxide with DNA-modified gold nanoparticles to develop a novel colorimetric sensing platform, Part. Part. Syst. Charact. 31 (2014) 201–208.
[21] N. Haghnazari, A. Alizadeh, C. Karami, Z. Hamidi, Simple optical determination of silver ion in aqueous solutions using benzo crown-ether modified gold nanoparticles, Microchim. Acta 180 (2013) 287–294.
[22] Y. Zhang, H. Jiang, X. Wang, Cytidine-stabilized gold nanocluster as a fluorescence turn-on and turn-off probe for dual functional detection of Ag^+ and Hg^{2+}, Anal. Chim. Acta 870 (2015) 1–7.
[23] W. Bian, H. Zhang, Q. Yu, M. Shi, S. Shuang, Z. Cai, M.M. Choi, Detection of Ag^+ using graphite carbon nitride nanosheets based on fluorescence quenching, Spectrochim. Acta A 169 (2016) 122–127.
[24] A. Ono, S. Cao, H. Togashi, M. Tashiro, T. Fujimoto, T. Machinami, S. Oda, Y. Miyake, I. Okamoto, Y. Tanaka, Specific interactions between silver (I) ions and cytosine-cytosine pairs in DNA duplexes, Chem. Commun. 39 (2008) 4825–4827.
[25] C. Zhao, K. Qu, Y. Song, C. Xu, J. Ren, X. Qu, A reusable DNA single-walled carbon-nanotube-based fluorescent sensor for highly sensitive and selective detection of Ag^+ and cysteine in aqueous solutions, Chem. Eur. J. 16 (2010) 8147–8154.
[26] H. Lv, S. Li, Y. Liu, G. Wang, X. Li, Y. Lu, J. Wang, A reversible fluorescent INHIBIT logic gate for determination of silver and iodide based on the use of graphene oxide and a silver–selective probe DNA, Microchim. Acta 182 (2015) 2513–2520.
[27] G. Wang, Y. Lu, C. Yan, Y. Lu, DNA-functionalization gold nanoparticles based fluorescence sensor for sensitive detection of Hg^{2+} in aqueous solution, Sens. Actuators B 211 (2015) 1–6.
[28] C. Hao, L. Xua, C. Xing, H. Kuang, L. Wang, C. Xu, Oligonucleotide-based fluorogenic sensor for simultaneous detection of heavy metal ions, Biosens. Bioelectron. 36 (2012) 174–178.
[29] Y. Liu, Y. Liu, Z. Li, J. Liu, L. Xu, X. Liu, An unusual red-to-brown colorimetric sensing method for ultrasensitive silver (I) ion detection based on a non-aggregation of hyperbranched polyethylenimine derivative stabilized gold nanoparticles, Analyst 140 (2015) 5335–5343.
[30] C.Y. Lin, C.J. Yu, Y.H. Lin, W.L. Tseng, Colorimetric sensing of silver (I) and mercury (II) ions based on an assembly of tween 20-stabilized gold nanoparticles, Anal. Chem. 82 (2010) 6830–6837.
[31] B. Li, Y. Du, S. Dong, DNA based gold nanoparticles colorimetric sensors for sensitive and selective detection of Ag (I) ions, Anal. Chim. Acta 644 (2009) 78–82.
[32] D.Q. Feng, G. Liu, W. Zheng, J. Liu, T. Chen, D. Li, A highly selective and sensitive on–off sensor for silver ions and cysteine by light scattering technique of DNA-functionalized gold nanoparticles, Chem. Commun. 47 (2011) 8557–8559.
[33] Y. Zhou, L. Tang, G. Zeng, J. Zhu, H. Dong, Y. Zhang, Y. Deng, A novel biosensor for silver (I) ion detection based on nanoporous gold and duplex-like DNA scaffolds with anionic intercalator, RSC Adv. 5 (2015) 69738–69744.
[34] P. Miao, L. Ning, X. Li, Gold nanoparticles and cleavage-based dual signal amplification for ultrasensitive detection of silver ions, Anal. Chem. 85 (2013) 7966–7970.
[35] L.M. Demers, C.A. Mirkin, R.A. Mucic, R.L. Reynolds, R. Letsinger, R. Elghanian, G. Viswanadham, A fluorescence-based method for determining the surface coverage and hybridization efficiency of thiol-capped oligonucleotides bound to gold thin films and nanoparticles, Anal. Chem. 72 (2000) 5535–5541.
[36] B. Ye, B. Yin, Highly sensitive detection of mercury (II) ions by fluorescence polarization enhanced by gold nanoparticles, Angew. Chem. Int. Ed. 47 (2008) 8386–8389.
[37] Y. Jiang, J. Tian, K. Hu, Y. Zhao, S. Zhao, Sensitive aptamer-based fluorescence polarization assay for mercury (II) ions and cysteine using silver nanoparticles as a signal amplifier, Microchim. Acta 181 (2014) 1423–1430.
[38] Q. Yue, T. Shen, L. Wang, S. Xu, H. Li, Q. Xue, Y. Zhang, X. Gu, S. Zhang, J. Liu, A convenient sandwich assay of thrombin in biological media using nanoparticle-enhanced fluorescence polarization, Biosens. Bioelectron. 56 (2014) 231–236.
[39] Y. Huang, X. Liu, L. Zhang, K. Hu, S. Zhao, B. Fang, Z. Chen, H. Liang, Nicking enzyme and graphene oxide-based dual signal amplification for ultrasensitive aptamer-based fluorescence polarization assays, Biosens. Bioelectron. 63 (2015) 178–184.